Armin Müller*, Ekaterina Kovacheva, Marc Alexander Fritz, Olaf Dössel, and Axel Loewe

Validating a Numerical Simulation of Human Heart Motion Using Clinical Data

Abstract: Numerical simulations are increasingly often involved in developing new and improving existing medical therapies. While the models involved in those simulations are designed to resemble a specific phenomenon realistically, the results of the interplay of those models are often not sufficiently validated. We created a plugin for a cardiac simulation framework to validate the simulation results using clinical MRI data. The MRI data were used to create a static whole-heart mesh as well as slices from the left ventricular short axis, providing the motion over time. The static heart was a starting point for a simulation of the heart's motion. From the simulation result, we created slices and compared them to the clinical MRI slices using two different metrics: the area of the slices and the point distances. The comparison showed global similarities in the deformation of simulated and clinical data, but also indicated points for potential improvements. Performing this comparison with more clinical data could lead to personalized modeling of elastomechanics of the heart.

Keywords: Simulation validation, numerical simulation, clinical data, motion deformation, human heart

1 Introduction

Despite a decrease in mortality of cardiovascular diseases, they are still the most common cause of death in Germany [1]. Therefore, finding and improving therapies is a major goal of many researchers.

Simulation frameworks support researchers and clinicians in developing and improving medical therapies but need to be verified and validated. Land et al. conducted a verification study on cardiac mechanics simulation software in 2015. They, as well as others, defined verification as "determining how accurate a computer program solves the equations of a mathematical model" and validation is defined as "determining how well a mathematical model represents the real world phenomena it is intended to predict" [2].

The aim of this work is to compare elastomechanical simulation results with clinical data quantitatively and answer the question to what extent can we validate a cardiac simulation with clinical data. In particular, the clinical data used in this work provide the deformation of the left ventricle over time.

2 Methods

2.1 Numerical Simulation Framework

The cardiac simulation framework that was used to perform the validation was CardioMechanics [3]. It was developed at the Institute of Biomedical Engineering (IBT) at Karlsruhe Institute of Technology (KIT). This framework uses the finite element method to simulate the beating of the human heart.

2.1.1 Geometry

The numerical simulation was performed on a whole-heart geometry consisting of 7623 points and 42282 tetrahedral volume elements of a heart in end-diastolic state.
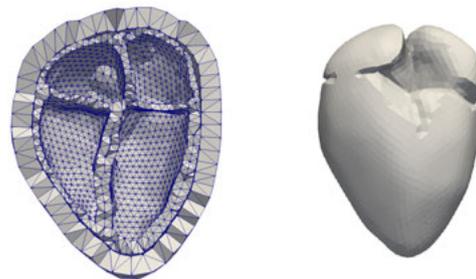
Fig. 1: The whole-heart geometry used for the simulation. On the left is the mesh of the heart clipped in the longitudinal axis. The thick layer with the coarser mesh surrounding the four chambers is the pericardial layer. Pictured on the right is the heart without the pericardial layer.

The geometrical mesh was created from magnetic resonance imaging (MRI) data of a healthy 40 year old male volunteer. The MRI data were provided by the University Hospital Heidelberg. The whole-heart geometry comprises the four

*Corresponding author: Armin Müller, Institute of Biomedical Engineering, Karlsruhe Institute of Technology (KIT), Kaiserstr. 12, 76131 Karlsruhe, Germany, e-mail: publications@ibt.kit.edu
Ekaterina Kovacheva, Marc Alexander Fritz, Olaf Dössel, Axel Loewe, Institute of Biomedical Engineering, Karlsruhe Institute of Technology (KIT), 76131 Karlsruhe, Germany

chambers of a human heart (left and right atrium and left and right ventricle) as well as a layer that mimics the pericardium as shown in Figure 1.
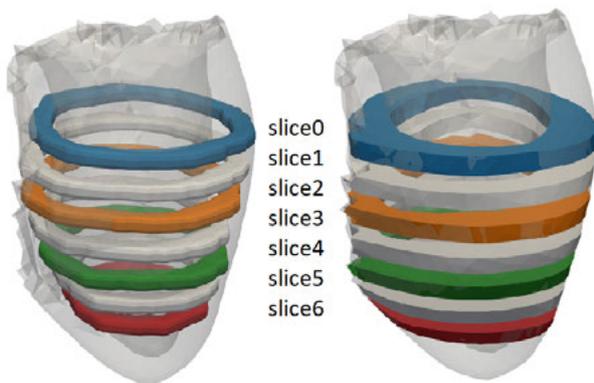
2.1.2 Simulation

CardioMechanics calculates the deformation of the input geometry that results from the interplay of the active and passive forces in the numerical model [3]. The underlying physics of cardiac biomechanics are described by the governing equation for the balance of linear momentum, which reduces to the equilibrium equation when mass inertia is neglected [4].

Here, the numerical model used for the active tension was the model proposed by Stergiopulos et al. [5], while for the passive material properties the transversely isotropic model proposed by Guccione et al. [6] was used. Since the patient's pulse was 50 bpm at the time of the MRI acquisition, we used 1.2 s as the heartbeat cycle length. For the evaluation, we used the simulation's fifth heartbeat to ensure that the simulation and the circulatory system model are in a steady state.

2.2 Data Generation

The MRI data consisted of 639 images with a resolution of 256x256 px. 455 of those images were left ventricular short axis images, distributed over nine slice planes, 40 showed the ventricular long axis with two chambers, and 35 the ventricular long axis with four chambers. The last 109 images were whole-heart images.

Fig. 2: On the left are the slices generated from the MR images. The right part of the image shows the slices generated from the simulation. On both sides, the simulated left ventricle is shown in transparent grey. The colors of slice0, slice2, slice4, and slice6 correspond to the colors used in later plots.

After the short axis images were manually segmented (ITK-SNAP, www.itksnap.org), surface meshes were created. Since at first we observed an intra-slices shift, we aligned the short axis slices based on the long axis slices. Furthermore, the orientation of the slices was aligned to the whole-heart geometry used for the simulation.

The aligned MRI slices were used as a ground truth and are compared to slices created synthetically from the whole-heart simulation. The simulation slices and the MRI slices were aligned at the peak systole (at 500 ms).

Since only the slice meshes for the left ventricle were available, we validated only the deformation of the left ventricle at 34 time points across one heartbeat.

2.3 Comparison Plugin

We implemented a plugin for CardioMechanics that compares the slices created from the MR images and those created from a simulation. The slices created from the MR images are an input for the plugin.

After the simulation is finished, the plugin creates the slices from the simulation results automatically. We decided to use the seven middle slices generated from the MR images and we named them slice0 (nearest to the heart's base) to slice6 (nearest to the heart's apex) as shown in Figure 2.

The plugin computes two different metrics on the corresponding slices: the total area of the slice surface and the Hausdorff metric of the mesh of the slices.

The area is calculated for both slices of each pair. The result was normalized to each slice's maximum during the cycle to compare the development of the area independently of its absolute value. After that, we calculated the difference e between the areas of the slices with $e = (area_A - area_B)$, where A and B are the two slices that are compared.

The Hausdorff metric, also called Hausdorff distance, measures the distance $d(A, B)$ between two non-empty compact subsets A, B of a metric space E. It is defined as the greatest of all distances from a point in the first subset to the closest point in the second subset [7].

To calculate the distance between two non-empty subsets, the distance δ between a point x and a non-empty compact set $K \subseteq E$ is defined as $\delta(x, K) := inf\{D(x, k)|k \in K\}$, where D is a metric of space E. The directed Hausdorff distance (dHDD) between two non-empty compact subsets $A, B \subseteq E$ is defined as $d_{dHDD}(A, B) = sup\{\delta(a, B)|a \in A\}$. Since dHDD is not symmetric, the Hausdorff distance (HDD) is defined as $d_{HDD}(A, B) = max\{d_{dHDD}(A, B), d_{dHDD}(B, A)\}$.

To obtain more evaluations from the comparison with the HDD, we divided each slice into four sections: the top, the bot-
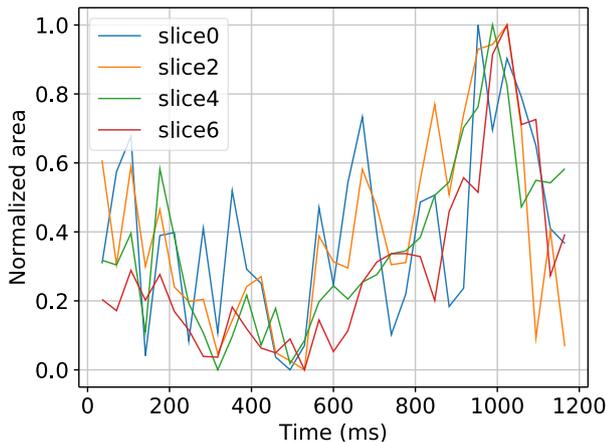
tom, the endocardial and the epicardial face. Thus, we obtain four comparison values per slice instead of one.

3 Results

In Figure 3 and 4, we show the normalized area of the slices during one heartbeat.
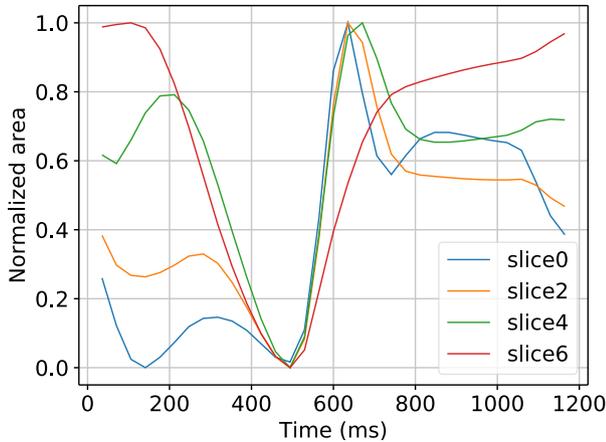
Fig. 3: Normalized surface area of the slices generated from the simulation.


Fig. 4: Normalized surface area of the slices generated from the MR images.

Figure 3 shows that for slice0 (between 0 and 70 ms), slice2 (between 0 and 130 ms), and slice4 (between 0 and

150 ms), the surface area initially decreased. After that, the area of those three slices increased. Shortly after that, the area for all slices started decreasing until they reached their minimum in the peak systole at 500 ms. The peak systole was defined to be the point of maximum contraction. Directly after the peak systole, there was an increase of the area up to the slice area's maximum (at 650 ms for slice0, slice2, and slice4) followed by a decrease (up to 750 ms) and a phase with small changes until the end of the heartbeat. Slice6 showed a different behavior. After reaching the minimum in the peak systole, its area increased until the end of the heartbeat.

In Figure 4, the surface area of the corresponding slices generated directly from the MR images is shown. The plots were aligned in time so that the peak systole in both plots appear at the same time, at 500 ms. In this plot, the initial decrease of the slice area is visible (at 320 ms) but it appears later compared to the simulation slices. After that, an increase of the area followed by a decrease up until the peak systole is visible. After the peak systole, there is an increase of the area up to its maximum at 1000 ms. While the simulation slices showed a decrease and a plateau phase after reaching the area's maximum, the MRI slices showed a decrease of the area until the end of the heartbeat.
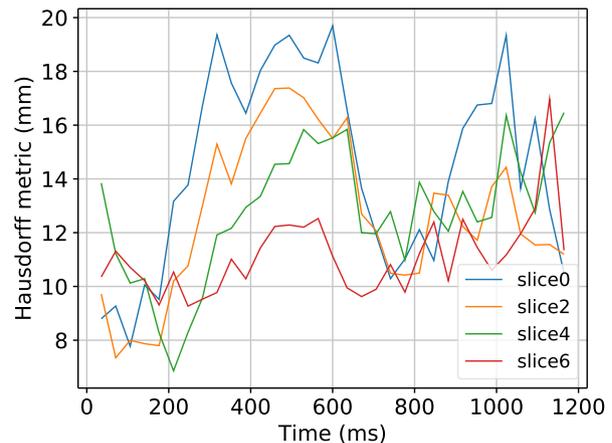
Fig. 5: The Hausdorff metric for the endocardial part of the slices.

Figure 5 shows the results of the Hausdorff metric over the course of one heartbeat for the endocardial part of the slices. The four different parts of the slices show a very similar behavior for the HDD allowing us to omit the plots for the other three parts. Figure 5 shows that slice2, slice4, and slice6 reach their maximum distance at peak systole (500 ms). The HDD of 20 mm is 26% of the ventricle diameter of 77 mm. After that, we observed a plateau phase (750 – 950 ms). This was followed by an increase of the HDD and finally a decrease at the

end of the heartbeat. Slice0 showed a plateau-phase from 750 to 850 ms followed by an increase and a drop of the distance at the end of the heartbeat.

4 Discussion

The surface area of the slices is affected by two factors: the wall thickness and the slice diameter. Until peak systole, the area of both slice sets decreases and after peak systole, the area of both sets increases. This indicates global similarities between both slice sets.

The initial decrease of the surface area is due to the decrease of the diameter while the wall thickness is rather constant. The increase of the area in the following 150 ms is caused by the thickening of the wall. After that, the wall thickening continues while the slice's diameter further decreases, so that the area also decreases until peak systole. In the future, we plan to quantify the diameter and radius changes. For the simulation slices, we can then observe an increase in the area until it reaches its maximum at 650 ms due to the continuing wall thickening. The maximum of the area for the MRI-slices is reached significantly later, at 1000 ms. The simulation slices show a plateau phase during the relaxation phase until the end of the heartbeat (750 ms – 1200 ms) because of two compensating factors: the thinning of the wall and the increasing of the diameter.

The ventricle's deformation during the systole between the MRI and the simulation slices are different. Both, the change of wall thickening as well as the change in diameter are less prominent for the MRI slices. Therefore, the HDD is increasing. After the systole, the HDD for slice2, slice4, and slice6 reach a plateau-phase due to the increase of the diameter that compensates the thinning of the wall. The observed differences might be due to a non-optimal choice of material parameters for the ventricle. Therefore, this comparison method can be included in an optimization framework which will determine optimal parameters for the material law so that the simulated deformation matches the one obtained from clinical data.

For the HDD, the closest point was found by selecting the nearest neighbor from the other set. Selecting the intersection of the normal of one point with the mesh of the other data-set might improve results.

There were 34 time points per heartbeat available for the creation of the MRI slices. For a thorough comparison, more time points would be desirable. The manual segmentation of the slices from the MR images is observer-dependent [8].

Selecting different slices also impacts the validation results.

5 Conclusion

In this work, we introduced a metric-driven approach to validate the deformation of a simulation of the human heart based on clinical data. The results showed that the validation of a cardiac simulation using clinical data requires further effort. We could observe only global similarities between the simulation and the MRI slices. Nevertheless, the comparison also showed that especially the relaxation phase between the simulation and the clinical data differ markedly for this volunteer.

References

[1] German Heart Report 2018. https://dgk.org

[2] S. Land, V. Gurev, S. Arens, et al., "Verification of cardiac mechanics software: benchmark problems and solutions for testing active and passive material behaviour," Proceedings. Mathematical, Physical, and Engineering Sciences / the Royal Society, vol. 471, no. 2184, p. 2015.0641, 2015.

[3] T. Fritz, C. Wieners, G. Seemann, et al., "Simulation of the contraction of the ventricles in a human heart model including atria and pericardium: Finite element analysis of a frictionless contact problem," Biomechanics and Modeling in Mechanobiology, vol. 13, no. 3, pp. 627–641, 2014.

[4] T. Belytschko, W. K. Liu, and B. Moran, "Nonlinear Finite Elements for Continua and Structures," Chichester: John Wiley and Sons, Ltd, 2000.

[5] N. Stergiopulos, et al., "Determinants of stroke volume and systolic and diastolic aortic pressure," Am J Physiol Heart Circ Physiol, vol. 270, no. 6, pp. H2050–H2059, 1996.

[6] J. M. Guccione, A. D. McCulloch, and L. K. Waldman, "Passive material properties of intact ventricular myocardium determined from a cylindrical model," J. Biomechanical Engineering, vol. 113, no. 1, pp. 42–55, 1 1991.

[7] F. Hausdorff, "Grundzüge der Mengenlehre". Verlag von Veit und Comp, 1914.

[8] S. E. Luijnenburg, D. Robbers-Visser, A. Moelker, et al., "Intra-observer and interobserver variability of biventricular function, volumes and mass in patients with congenital heart disease measured by CMR imaging," Int J Cardiovasc Imaging, vol. 26, pp. 57–64, 2010.